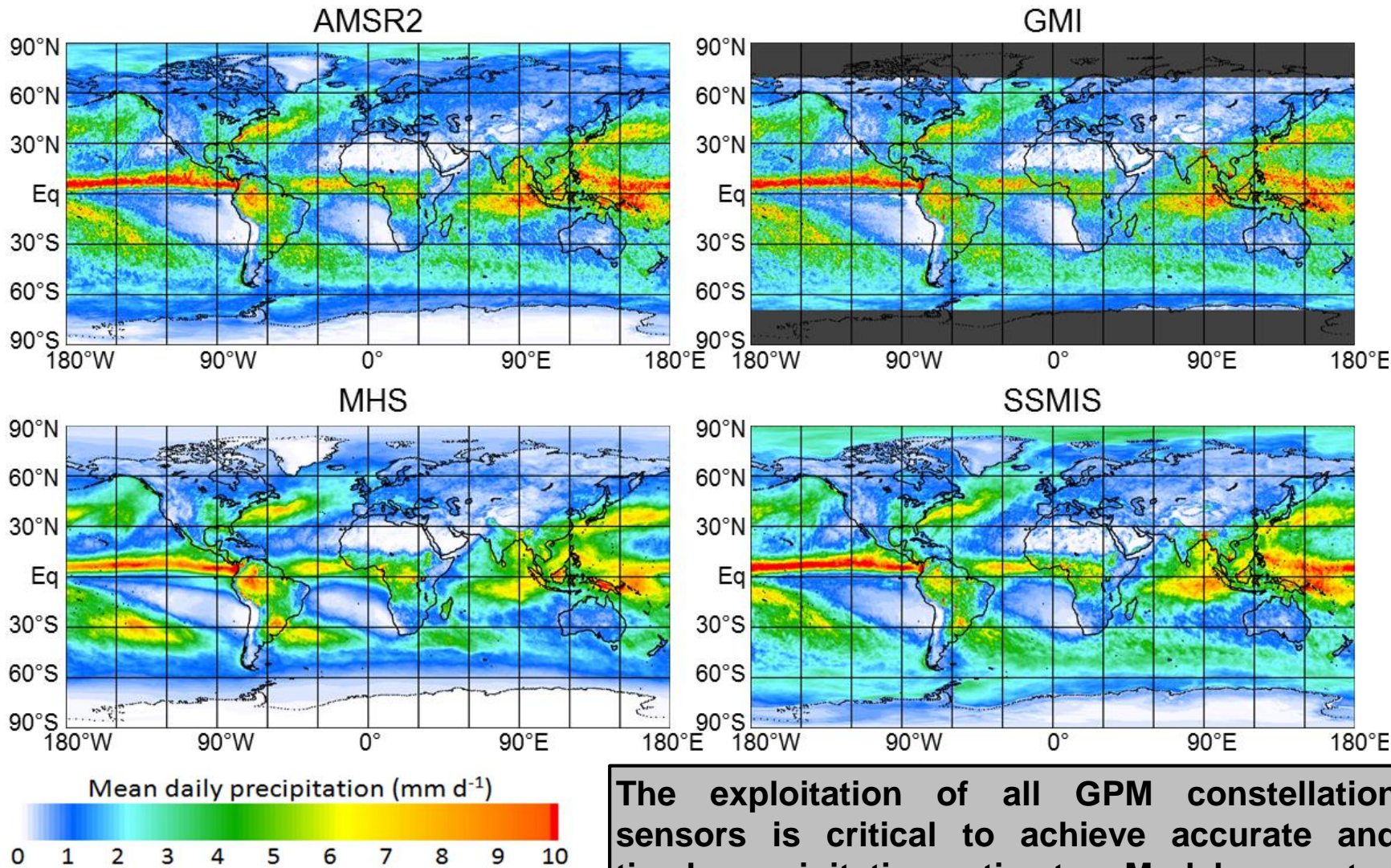# Exploiting the full GPM constellation for the retrieval of precipitation

C Kidd[1,2*], T Matsui[1,2], J Chern[1,2], K Mohr[3], C Kummerow[4] and D Randel[4],
[1]Code 612, NASA/GSFC, [2]UMD/ESSIC, [3]Code 610, NASA/GSFC, [4]Colorado State University

Mean daily precipitation (mm d^{-1})

Mean daily rainfall
6 March 2014 – 5 March 2015

The exploitation of all GPM constellation sensors is critical to achieve accurate and timely precipitation estimates. Model-generated databases allow cross-track sensors to be fully utilized for global precipitation measurements.

Earth Sciences Division - Atmospheres

Name: Chris Kidd, NASA/GSFC, Code 612 and University of Maryland/ESSIC
E-mail: chris.kidd@nasa.gov
Phone: 301-614-6091

References:

Chris Kidd, Toshihisa Matsui, Jiundar Chern, Karen Mohr, Chris Kummerow, and Dave Randel, 2016: Global Precipitation Estimates from Cross-Track Passive Microwave Observations Using a Physically Based Retrieval Scheme. *Journal of Hydrometeorology*, **17**, 383–400. doi: 10.1175/JHM-D-15-0051.1

Data Sources:

Kidd, C. 2014a: last updated 2014: GPROF NOAA-18 MHS Level 2A precipitation product. NASA/GSFC, Greenbelt, MD, USA. doi=10.5067/GPM/MHS/NOAA18/GPROF2A

Kidd, C. 2014b: last updated 2014: GPROF NOAA-19 MHS Level 2A precipitation product. NASA/GSFC, Greenbelt, MD, USA. doi=10.5067/GPM/MHS/NOAA19/GPROF2A

Kidd, C. 2014c: last updated 2014: GPROF EUMETSAT MetOpA MHS Level 2A precipitation product. NASA/GSFC, Greenbelt, MD, USA. doi=10.5067/GPM/MHS/METOPA/GPROF2A

Kidd, C. 2014d: last updated 2014: GPROF EUMETSAT MetOpB MHS Level 2A precipitation product. NASA/GSFC, Greenbelt, MD, USA. doi=10.5067/GPM/MHS/METOPB/GPROF2A
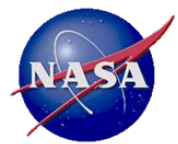
Kidd, C. 2015: last updated 2015: GPROF CNES/ISRO Megha Tropiques SAPHIR radiometer GPROF Precipitation Retrieval Level 2A precipitation product. NASA/GSFC, Greenbelt, MD, USA. doi=10.5067/GPM/SAPHIR/MT/GPROF2A

Technical Description of Figure:

Mean Daily Rainfall: Comparison of the mean daily precipitation estimates generated for four different satellite sensors within the Global Precipitation Measurement (GPM) mission constellation for 6 March 2014 through 5 March 2015. The Advanced Microwave Scanning Radiometer-2 (AMSR2; *upper left*), GPM Microwave Imager (GMI; *upper right*) and Special Sensor Microwave Imager-Sounder (SSMIS; *lower right*) products are derived from conically-scanning sensors that have formed the mainstay of satellite precipitation retrievals for the last 30 years. The ability to exploit observations from cross-track sensors is critical to achieve the temporal sampling needed for accurate precipitation retrievals. Challenges associated with incorporating these cross-track sensors into the GPM constellation were overcome by utilizing information gained from models to construct a suitable database used in the retrieval scheme. The mean daily rainfall derived from the cross-track Microwave Humidity Sounder (MHS, *lower left*) illustrates the ability of the cross-track sensors to provide precipitation estimates similar to those derived from the conically-scanning sensors. Some differences between the products do exist, notably at high latitudes where the ASMR2 and SSMIS products are too high due to contamination by surface ice-melt, and in the South Pacific mid-latitudes where the MHS product shows higher mean daily precipitation.

Scientific significance, societal relevance, and relationships to future missions:
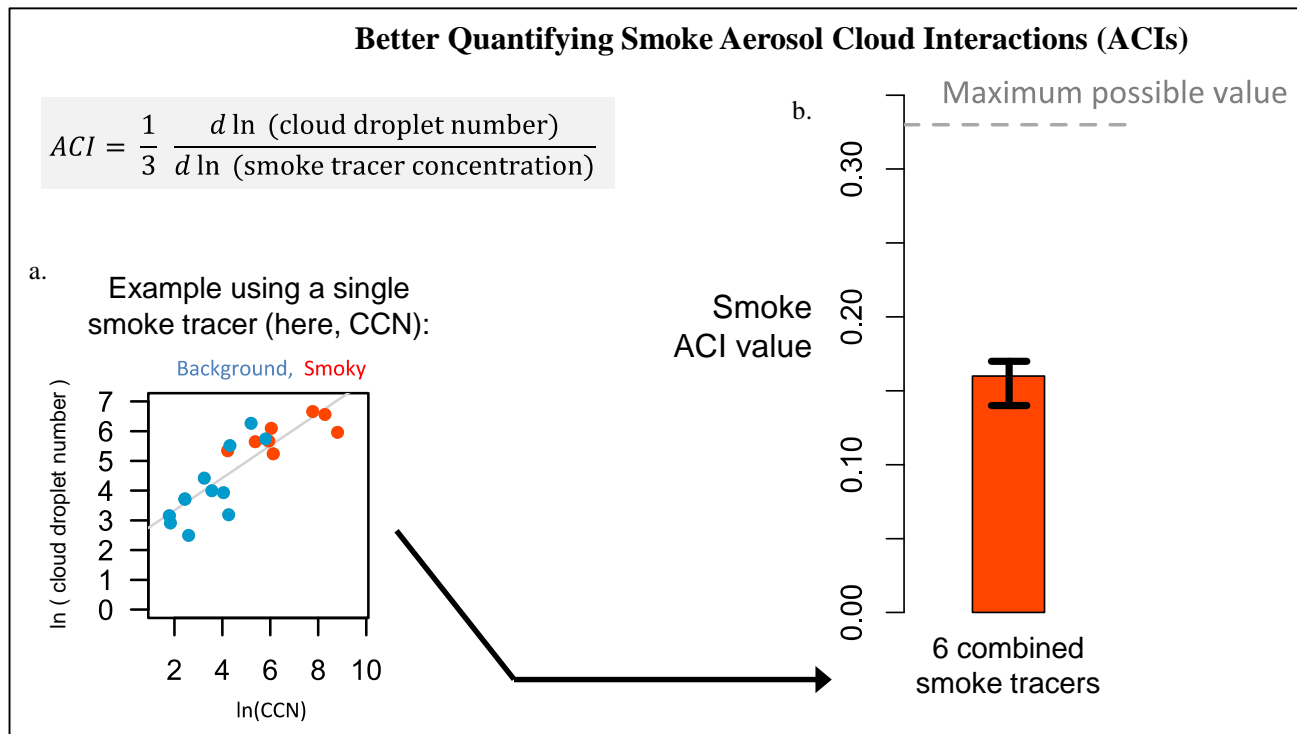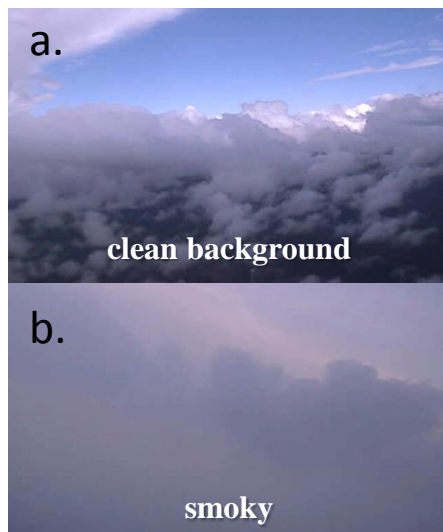
The GPM mission, launched in February 2014, provides a greatly enhanced system for the measurement of precipitation on a global scale. Through improved instrumentation on the GPM Core Observatory together with international partner satellites and sensors observations can be generated globally every 3 hours better than 90% of the time, and ultimately 30 minute estimates with the integration of infrared data. Historically the conically-scanning passive microwave radiometers (imagers) have been the mainstay of observations for precipitation estimates, but cross-track sensors ('sounders') also have the capability to provide precipitation retrievals. The inclusion of the cross-track sensors within the GPM constellation is key to achieving the >90% revisit time. Moreover, with the demise of the Tropical Rainfall Measuring Mission (TRMM) and the Defense Military Satellite Program (DMSP) F19 satellite, the cross-track sensors now form the majority of precipitation-capable sensors. The gradual erosion of conically-scanning sensors will certainly continue in the coming years due to the age of current sensors. No future launches of conically-scanning sensors are planned before that of the European Polar System Second Generation (EPS-SG) MicroWave Imager (MWI) in 2023.

Earth Sciences Division - Atmospheres

Aircraft observations help quantify smoke microphysical impacts on Arctic and subarctic clouds

L. Zamora[1,2], R. Kahn[1]

[1]Code 613, NASA/GSFC, [2]USRA

Better Quantifying Smoke Aerosol Cloud Interactions (ACIs)

$$ACI = \frac{1}{3} \frac{d \ln (\text{cloud droplet number})}{d \ln (\text{smoke tracer concentration})}$$

a.
Example using a single smoke tracer (here, CCN):

Background, Smoky

a.
clean background

b.
smoky

Smoke ACI value

Maximum possible value

6 combined smoke tracers

Aircraft data were used to compare cloud properties in smoky and background aerosol conditions in the Arctic and subarctic. These relationships are used to better quantify the response of Arctic/subarctic clouds to smoke aerosols (e.g., see above). Our results are complementary to remote sensing observations. They also allow direct parameterization and validation of models and enable better estimation of summertime short-wave radiative flux.

Name: Lauren Zamora, NASA/GSFC, Code 613 and USRA
E-mail: lauren.m.zamora@nasa.gov
Phone: 301-614-6353

Reference:

Data Sources:

Technical Description of Figures:
Left figure: Examples from the ARCTAS aircraft campaign of (a) sampled clean "background" clouds, and (b) smoky clouds.
Right figure: (a) Multi-campaign data showing an example of how the aerosol cloud interaction (ACI) parameter value is calculated based on a single smoke tracer (here cloud condensation nuclei (CCN) concentration). (b) We combined 6 biomass burning tracers to estimate that smoke aerosols increase median cloud droplet number by ~half of the possible maximum (0.16 out of 0.33), a phenomenon that was known but not well quantified, especially at high latitudes. Of particular significance in this work is the careful characterization of background clouds. Note: in concentrated smoke plumes where water vapor competition is high, impacts were substantially lower (data not shown; see Zamora et al., 2016).

Scientific significance, societal relevance, and relationships to future missions:
The Arctic is experiencing a series of rapid environmental changes. Currently, our ability to predict future changes is hampered, in part, by a poor understanding of Arctic cloud-aerosol interactions, which affect the radiation budget. At the same time, Arctic and subarctic wildfires are increasing due to the changing climate, and might double or triple by the end of the century. Smoke is believed to have a large effect on cloud lifetime, albedo, and precipitation. However, the interactions between smoke particles and clouds remain poorly quantified due to confounding meteorological influences, remote sensing limitations and biases (which are particularly high in the Arctic), and limited *in situ* observations. Here, we pulled together data from multiple historic aircraft campaigns in the Arctic and subarctic to reduce these uncertainties. Smoke halved median cloud droplet radius in liquid clouds. In some summertime low-albedo conditions, we estimate that smoke-driven cloud indirect effects may decrease surface shortwave fluxes by 2-4 W m^{-2} or more. These findings will be useful input for radiative transfer models, and for constraining the energy balance in a changing Arctic. Moreover, they will enhance the utility of remote sensing observations, which show trends in clouds very well, but which, without context from *in situ* studies, can underestimate cloud albedo effects. Information from our study highlights the need to continue improvements to satellite retrievals of aerosol and cloud properties in polar regions.
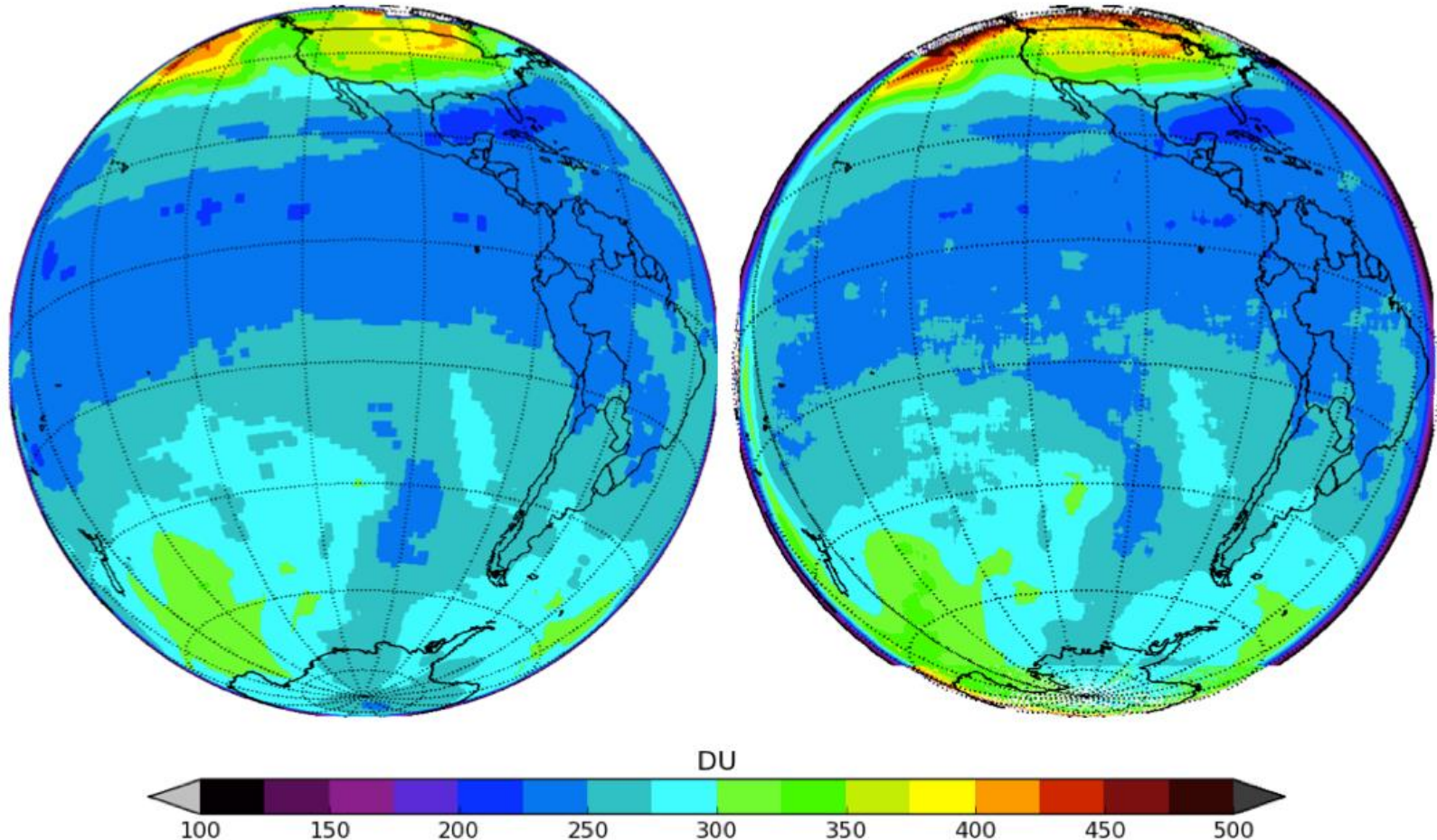
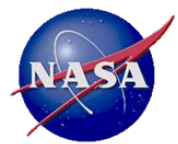**Earth Sciences Division - Atmospheres**

Total Ozone Comparison between SNPP/OMPS and DSCVR/EPIC Ozone

Jay Herman, Code 614, NASA/GSFC (and UMBC/JCET)

OMPS Nadir Mapper
10 January 2016

EPIC
10 January 2016, 200622

DU

100   150   200   250   300   350   400   450   500

The image on the left is a traditional composite of multiple orbits of Suomi NPP data taken over a 24 hour period. The image on the right is a snapshot taken by the EPIC instrument on the DSCOVR satellite at 20:06 GMT observing from the L1 point.

Earth Sciences Division - Atmospheres

Name: Point of Contact, Jay Herman NASA/GSFC, Code 614 (and UMBC/JCET)
E-mail: jay.r.herman@nasa.gov
Phone: 301-614-6039

References:
A preliminary version of these results were presented at the 2015 December AGU meeting

Data Sources: EPIC UV Data processed by the EPIC/DSCVR Team at NASA/GSFC (Key contributors: Dr Colin Seftor, Dr. Jay Herman, Karin Blank)

Technical Description of Figures:
The global distribution of ozone on January 10, 2016 obtained from EPIC at 50 x 50 km^2 spatial resolution (right) using newly calibrated 325 and 340 nm measured radiances compared to the ozone field obtained from Suomi/OMPS (left). Almost identical ozone results have been obtained using 317.5 nm and 340 nm. Since each filter measurement/image is obtained at slightly different times, considerable effort was required for geolocating the images so that corresponding pixels from each filter were looking at the same scene. Since OMPS measures at 13:30±1 hour, the global OMPS image is stitched together from narrow strips, while the EPIC image represents the instantaneous ozone amounts from sunrise in the west to sunset in the east.
I

Scientific significance, societal relevance, and relationships to future missions:
We have obtained estimates for the calibration coefficients K(317.5), K(325 nm) and K(340 nm) that yielded an improved (right) ozone retrieval that has been compared with the same day as observed from Suomi/OMPS (left). The calibration estimates will be improved with a goal of 2% ozone accuracy (currently at 5%). The native spatial resolution from EPIC $20 \times 20 \text{ km}^2$ has been reduced to approximate the $50 \times 50 \text{ km}^2$ resolution from OMPS. While the agreement appears to be quite good, there are issues at high solar zenith and view angles in both the latitude and longitude directions that are not present in the nadir viewing OMPS data. Additional work is required developing retrieval algorithms incorporating improved spherical geometry calculations and improved calibration coefficients K for each wavelength.

Based on the results obtained with the preliminary retrieval algorithm, a production algorithm for calculating ozone, Lambert Equivalent Reflectivity (LER), aerosol index, and aerosol optical depth from the 317.5, 325, 340, and 388 nm channels must to be developed for the special geometry needed for analysis of EPIC data. In particular, we need to understand and eliminate the small, but significant, bias between 340 nm LER and 388 nm LER. The derived EPIC data must be compared extensively with results from well-established results from OMI and OMPS obtained at 13:30 local time. Most interesting are the EPIC ozone "movies" we have obtained showing the motions of ozone during the day, especially the rotation of the Antarctic Ozone Hole as it passes over the tip of South America. This is important for understanding the amount of time people are exposed to enhanced levels of UV radiation from reduced ozone amounts. This result is not available from low earth orbiting (LEO) satellites such as OMI or OMPS.

While not shown here, the ozone results combined with the O2 A-band observations enable EPIC to "see" clouds over ice. The combination leads to improved estimates of solar energy reaching the ice surface leading to melting, an important climate parameter.
.

Earth Sciences Division - Atmospheres